

How quantum are classical spin ices?

Jeffrey G. Rau¹ and Michel J. P. Gingras^{1,2,3}

¹*Department of Physics and Astronomy, University of Waterloo, Ontario, N2L 3G1, Canada*

²*Perimeter Institute for Theoretical Physics, Waterloo, Ontario, N2L 2Y5, Canada*

³*Canadian Institute for Advanced Research, 180 Dundas Street West, Suite 1400, Toronto, ON, M5G 1Z8, Canada*

The pyrochlore spin ice compounds $\text{Dy}_2\text{Ti}_2\text{O}_7$ and $\text{Ho}_2\text{Ti}_2\text{O}_7$ are well described by classical Ising models down to very low temperatures. Given the empirical success of this description, the question of the importance of quantum effects in these materials has been mostly ignored. We show that the common wisdom that the strictly Ising moments of Dy^{3+} and Ho^{3+} imply strictly Ising interactions is too naïve; a more complex argument is needed to explain the close agreement between theory and experiment. From a microscopic picture of the interactions in rare-earth oxides, we show that the high-rank multipolar interactions needed to induce quantum effects are generated only very weakly by super-exchange. Using this framework, we formulate an estimate of the scale of quantum effects in $\text{Ho}_2\text{Ti}_2\text{O}_7$ and $\text{Dy}_2\text{Ti}_2\text{O}_7$, finding it to be well below experimentally relevant temperatures. We discuss the implications of these results for realizing quantum spin ice in other materials.

Introduction: Spin ice has proven to be one of the more fruitful marriages of theoretical and experimental condensed matter physics [1–5]. This cooperative paramagnetic [6] phase is a magnetic analogue of common water ice [1, 2], with proton displacements mapped to magnetic moments pointing in or out of the corner-shared tetrahedra of the pyrochlore lattice [7]. Spin ice displays an exponential number of low-energy states, and thus an associated extensive residual entropy [8, 9]. This manifold is characterized by the ice rules specifying that on each tetrahedron two spins must point in, and two must point out. Generically referred to as a “Coulomb phase” [10, 11], the spin ice state harbors a rich phenomenology such as bow-tie shaped singularities (pinch points) in the magnetic structure factor [11, 12] and gapped low-energy excitations which provide a condensed matter realization of “magnetic monopoles” [4, 10].

The two textbook materials that realize this spin ice physics are the pyrochlore rare-earth titanates [3] $\text{Ho}_2\text{Ti}_2\text{O}_7$ [7] and $\text{Dy}_2\text{Ti}_2\text{O}_7$ [8]. Significant evidence has accumulated that their magnetic and thermodynamic properties [10, 13–15] can be quantitatively described by a classical model that includes nearest-neighbor exchange and long-range magnetostatic dipole-dipole interactions, both of *purely* Ising type. Amendments incorporating Ising interactions beyond nearest-neighbors have been proposed to account for various fine details in the thermodynamic and magnetic behavior of $\text{Dy}_2\text{Ti}_2\text{O}_7$ [14, 16, 17]. The combination of Ising exchanges and long-range dipolar interactions is expected to lift the degeneracy of the ice manifold and release the residual entropy at very low temperatures [18–21]. Experimentally, such a transition has yet to be observed [22], with further significant deviations [23] from predictions raising questions to the completeness of the classical dipolar Ising spin-ice model [16]. In particular, one could speculate that the observed rise of the magnetic specific heat below ~ 500 mK [23] is an indication that quantum effects are becoming important [24, 25].

This classical Ising description [13, 15, 26] of the interactions has framed the theoretical and experimental perspectives [1–5] on these materials dating back to their initial discovery [7, 8]. Beyond its empirical successes, this mind-set [13–

21, 26] is rooted in the *single-ion* magnetic properties of Dy^{3+} [22, 27–29] and Ho^{3+} [26, 30–32], specifically in the Ising nature of the crystal electric field (CEF) ground doublet. A consequence of this strict Ising anisotropy is that the transverse components of the total angular momentum, J^\pm , *vanish* between states of the CEF doublet. This is sufficient to explain the Ising form of any bilinear, anisotropic exchange interactions $\sim J_i^\mu K_{ij}^{\mu\nu} J_j^\nu$, including the long-range dipolar interactions [2]. The theoretical basis of the classical Ising description of spin ices then appears to rest on the implicit assumption that interactions between the rare-earth ions takes such a bilinear form. This common assumption is in fact *incorrect*; due the large spin-orbit coupling in rare-earth ions, strong multipolar interactions between the J_i^μ momenta are generated when the microscopic super-exchange is downfolded into the free-ion $2S+1L_J$ manifold [33]. Indeed, this argument has been invoked [34] to show that quadrupolar interactions may not be negligible in Pr-based pyrochlore oxides with strictly Ising moments, such as $\text{Pr}_2\text{Sn}_2\text{O}_7$ [35] and $\text{Pr}_2\text{Zr}_2\text{O}_7$ [36]. Further compounding the problem is the possibility that even moderate transverse couplings could preempt the ordering expected from the dipolar interactions. The existence of other spin ice compounds, such as $\text{Ho}_2\text{Sn}_2\text{O}_7$ [28, 37], $\text{Dy}_2\text{Sn}_2\text{O}_7$ [28, 38], $\text{Ho}_2\text{Ge}_2\text{O}_7$ [32, 39] and $\text{Dy}_2\text{Sn}_2\text{O}_7$ [29, 39] makes an explanation through some accidental fine-tuning unlikely. An unanswered puzzle thus lies in the identification of $\text{Dy}_2\text{Ti}_2\text{O}_7$ and $\text{Ho}_2\text{Ti}_2\text{O}_7$ as spin ices: Why are these compounds so well described by a classical Ising model down to low temperatures? What principles, if any, constrain the scale of the multipolar interactions and suppress significant quantum fluctuations?

In this letter, we explain why quantum effects in Dy- and Ho-based spin ice materials are small, providing approximate upper bounds on their size. First, we outline possible sources of exchange interactions and show that only magnetic dipole-dipole (MDD) and super-exchange between the rare-earth ions are potentially non-negligible at experimentally relevant temperatures. As the MDD interaction is purely Ising when projected into the ground CEF doublet, we focus on super-exchange. Using a microscopic model of the oxygen charge transfer processes, we find that the resulting multipolar

inter-ionic couplings arising from super-exchange are strongly suppressed beyond rank seven [40]. Because of the composition of the ground doublet, operators of rank seven or less can only connect its sub-leading spectral components and are thus highly suppressed. From experimental constraints on the size of these sub-leading components, we formulate estimates of the magnitude of the transverse (non-Ising) couplings in the low-energy theory, estimating them to be roughly two orders of magnitude smaller than the nearest-neighbor Ising coupling. To make this more concrete, we carry out a model calculation of the super-exchange interaction in $\text{Dy}_2\text{Ti}_2\text{O}_7$ and $\text{Ho}_2\text{Ti}_2\text{O}_7$. This calculation corroborates our argument and provides explicit estimates for the size of quantum effects in the $\text{Ho}_2\text{Ti}_2\text{O}_7$ and $\text{Dy}_2\text{Ti}_2\text{O}_7$ spin ices.

Since the arguments we follow for $\text{Dy}_2\text{Ti}_2\text{O}_7$ and $\text{Ho}_2\text{Ti}_2\text{O}_7$ are similar, we focus our presentation on $\text{Dy}_2\text{Ti}_2\text{O}_7$ and leave a detailed exposition of the results for $\text{Ho}_2\text{Ti}_2\text{O}_7$ to the Supplemental Material [41].

Pseudo-spin model: Our ultimate goal is to understand the interactions acting between the low energy states of the CEF manifold. In $\text{Dy}_2\text{Ti}_2\text{O}_7$ this is a Kramers doublet built from states in the ${}^6\text{H}_{15/2}$ manifold of the $4f^9$ configuration of Dy^{3+} . For a realistic CEF potential [30, 42], the ground state is a doublet with a gap of ~ 30 meV to the first excited level. This doublet transforms in the $\Gamma_5 \oplus \Gamma_6$ representation of the site symmetry group D_{3d} and has Ising-like character [43], as shown below. One writes the doublet states as

$$|\pm\rangle = \alpha \left| \pm \frac{15}{2} \right\rangle \pm \delta_1 \left| \pm \frac{9}{2} \right\rangle - \delta_2 \left| \pm \frac{3}{2} \right\rangle \mp \delta_3 \left| \mp \frac{3}{2} \right\rangle + \delta_4 \left| \mp \frac{9}{2} \right\rangle \pm \delta_5 \left| \mp \frac{15}{2} \right\rangle, \quad (1)$$

where $|M\rangle \equiv |15/2, M\rangle$ are eigenstates of the J^2 and J^z operators of the ${}^6\text{H}_{15/2}$ manifold. We choose the doublet basis so that $\delta_2\delta_3 - 3\delta_1\delta_4 + 5\alpha\delta_5 = 0$ to make the J^z dipole operator diagonal. The matrix elements of the magnetic dipole operators then take the form

$$\langle \sigma | J^\pm | \sigma' \rangle = 0, \quad \langle \sigma | J^z | \sigma' \rangle = \lambda \sigma \delta_{\sigma\sigma'}, \quad (2)$$

where $\sigma = \pm$ and the λ -factor is

$$\lambda \equiv \frac{15}{2} - 3 \left(\delta_1^2 + 2\delta_2^2 + 3\delta_3^2 + 4\delta_4^2 + 5\delta_5^2 \right). \quad (3)$$

Including the Dy^{3+} Landé factor $g = 4/3$, the magnetic moment $\mu = g\mu_B\lambda$ is found experimentally to be very close to maximal. Estimates from the saturation magnetization and high-temperature susceptibility [22, 27] give $\mu = (10 \pm 0.1) \mu_B$. This constrains the $|\pm\rangle$ states in Eq. (1) to be predominantly $|\pm 15/2\rangle$ [8, 30]. We thus have an upper bound of $\delta_n^2 \lesssim 0.025/n$ given $\pm 0.1 \mu_B$ error bars.

Since the CEF energy scale is large, it is sufficient to first consider only a bare projection of the microscopic Dy^{3+} - Dy^{3+} interactions acting within the full ${}^6\text{H}_{15/2}$ manifold into the ground doublet. Such a model can be expressed in terms of the components of a pseudo-spin 1/2 operator

$$S^\pm = |\pm\rangle \langle \mp|, \quad S^z = \frac{1}{2} (|+\rangle \langle +| - |-\rangle \langle -|). \quad (4)$$

The symmetry of the pyrochlore lattice constrains the form of any such projected Hamiltonian. The nearest-neighbor effective exchange model for $\text{Dy}_2\text{Ti}_2\text{O}_7$ is restricted to the form [43]

$$\sum_{\langle ij \rangle} \left[J_{xx} S_i^x S_j^x + J_{yy} S_i^y S_j^y + J_{zz} S_i^z S_j^z + J_{xz} (S_i^z S_j^x + S_i^x S_j^z) \right]. \quad (5)$$

Since the $J_{\mu\nu}$ are *not* bond dependent, the J_{xz} coupling can be removed by a global rotation of the pseudo-spin operators about the \hat{y} axis [43], yielding

$$\sum_{\langle ij \rangle} \left[J_x S_i^x S_j^x + J_y S_i^y S_j^y + J_z S_i^z S_j^z \right]. \quad (6)$$

We will find below that the net J_{zz} , including both the contribution from microscopic inter-ionic super-exchange and the nearest-neighbor MDD contribution, is the dominant coupling and that it is positive, as originally found empirically in Ref. [13]. At leading order, the rotated couplings are

$$J_x \sim J_{xx} - \frac{J_{xz}^2}{J_{zz}}, \quad J_y = J_{yy}, \quad J_z \sim J_{zz} + \frac{J_{xz}^2}{J_{zz}}. \quad (7)$$

This rotation affects the relationship between the components of the dipole moment and those of the pseudo-spin 1/2 at $O(J_{xz}/J_{zz})$. We characterize deviations from the Ising limit using the nearest-neighbor transverse scale $J_\pm \equiv (J_x + J_y)/4$ [43]. Our goal is to estimate the size of J_\pm and thus the strength of the quantum effects within the low-energy pseudo-spin 1/2 model.

Interactions in rare-earth pyrochlores: To understand how the microscopic inter-ionic coupling mechanisms generate J_\pm , we need to consider higher energy physics and a description beyond the lowest CEF doublet. At the atomic level, there is a hierarchy of energy scales for the rare-earth ions: the Coulomb interaction being largest, followed by spin-orbit coupling and the CEF potential. The Coulomb interaction plays two roles: it provides the repulsion that separates the different $4f^n$ charge states and splits each $4f^n$ manifold in approximate fixed orbital and spin angular momenta ${}^{2S+1}L$ [44]. Spin-orbit coupling then lifts the degeneracy of the states with the same total angular momentum J , giving the terms ${}^{2S+1}L_J$. Finally, the single-ion spherical symmetry of the ion is broken by the CEF and the ${}^{2S+1}L_J$ manifolds are further split into CEF multiplets.

We thus move one abstraction level up from the pure ground doublet, considering interactions within the ${}^6\text{H}_{15/2}$ manifold. Due to the spherical symmetry of the free ions, it is useful to categorize interactions and operators in terms of their *rank* as spherical tensors. Due to the large value $J = 15/2$ in the ${}^6\text{H}_{15/2}$ manifold of $\text{Dy}_2\text{Ti}_2\text{O}_7$, multipolar interactions up to rank-15 are possible [33]. Interactions at this level will typically be on the order of ~ 1 K, as inferred from the Curie-Weiss scale [7, 8]. Since the CEF energy scale is of order 300 K [30], it is sufficient to consider only the projection into the ground doublet. Perturbative corrections are then expected at second

order [45] with scale of $\sim (1 \text{ K})^2/300 \text{ K} \sim 3 \text{ mK} - 5 \text{ mK}$ and thus can be neglected. There are several sources of interactions between rare-earth ions: electro- and magnetostatic interactions, super-exchange, direct exchange, lattice-mediated exchange, etc. Of these the MDD and super-exchange interactions are found to be the most significant [41].

The long-range MDD interaction features prominently in classical spin ices [13–15, 26]. When projected into the ground doublet, it takes the form

$$\mathcal{D} \sum_{i < j} S_i^z S_j^z \left(\frac{r_{nm}}{r_{ij}} \right)^3 \left[\hat{z}_i \cdot \hat{z}_j - (\hat{r}_{ij} \cdot \hat{z}_i)(\hat{r}_{ij} \cdot \hat{z}_j) \right], \quad (8)$$

where r_{nm} is the nearest-neighbor distance between the rare-earth atoms, $\vec{r}_{ij} \equiv \vec{r}_i - \vec{r}_j$ is the displacement vector between the two sites and \hat{z}_i is the quantization axis along the local cubic [111] direction at site \vec{r}_i . The strength of the coupling is characterized by $\mathcal{D} = g^2 \lambda^2 \mu_B^2 \mu_0 / (4\pi r_{nm}^3)$. The largest piece is the nearest-neighbor contribution [16], with coefficient $D \equiv 5\mathcal{D}/3$ which is $\sim 8.9 \text{ K}$ in $\text{Dy}_2\text{Ti}_2\text{O}_7$ [46]. To obtain a quantitative agreement with experiments, corrections to the Ising couplings must be included. The nearest-neighbour correction J is the largest, estimated to be $\sim 4.96 \text{ K}$ in $\text{Dy}_2\text{Ti}_2\text{O}_7$ [13], later refined to $\sim 4.55 \text{ K}$ [16]. This coupling has usually been attributed to super-exchange processes between the rare-earth ions and provides an indication of their overall scale [47]. We are thus confronted with the question: with such a large scale, why does super-exchange not generate significant transverse couplings J_{\pm} ?

Oxygen-mediated super-exchange: To answer this question, we consider super-exchange interactions proceeding through the oxygen atoms that surround each rare-earth ion. To simplify our notation, we single out one exchange path consisting of two rare-earths and one oxygen. For the rare-earth sites, we define the creation operators $f_{1\alpha}^\dagger$ and $f_{2\alpha}^\dagger$ while for the intermediate oxygen site we use p_α^\dagger . A combined spin-orbital index $\alpha \equiv (m, \sigma)$ where m and σ label the orbital and spin quantum numbers is used throughout. Due to the localized nature of the rare-earth ions, we start with the atomic Hamiltonian at each site

$$H_0 \equiv H_{f,1} + H_{f,2} + H_p, \quad (9)$$

where $H_{f,1}$ and $H_{f,2}$ are the atomic Hamiltonian for the two rare-earth ions and H_p for the oxygen site. On the oxygen site, we consider only the atomic potential Δ_{pf} and the cost to place two holes together on the same oxygen, U_p . We will not invoke the details of the rare-earth atomic Hamiltonian, aside from selecting the ${}^6\text{H}_{15/2}$ manifold of the $4f^9$ configuration. We perturb H_0 with the hybridization terms

$$V \equiv \sum_{\alpha\beta} \left[t_{1,\alpha\beta} f_{1\alpha}^\dagger p_\beta + t_{2,\alpha\beta} f_{2\alpha}^\dagger p_\beta + \text{h.c.} \right], \quad (10)$$

that represent electron hopping between the orbitals of the rare-earth and oxygen ions. Super-exchange interactions are generated at fourth-order in perturbation theory in V [34]. For

the details of the charge-transfer processes, see the Supplemental Material [41].

To simplify the resolvents that appear in the perturbative expansion [41, 48], we follow Ref. [34] and make the common approximation that only the charging energies $E(f^{9\pm 1}) - E(f^9) \equiv U_f^\pm$ are significant. This neglects all other intra-atomic splittings on the rare-earth sites, such as those due to Hund's coupling or spin-orbit coupling. The energies U_f^\pm are expected to be of order $5 - 10 \text{ eV}$ in $4f$ compounds [49]. Within this approximation, the effective Hamiltonian can be written [34]

$$H_{\text{eff}} = \sum_{\alpha\beta\mu\nu} (P_1 f_{1\alpha}^\dagger f_{1\beta} P_1) \mathcal{I}_{12}^{\alpha\beta\mu\nu} (P_2 f_{2\mu}^\dagger f_{2\nu} P_2), \quad (11)$$

where P_i projects into the ground state manifold of $H_{f,i}$ at site i . The interaction matrix \mathcal{I} is defined as [41]

$$\mathcal{I}_{12}^{\alpha\beta\mu\nu} \equiv \frac{2}{(U_f^+ + \Delta_{pf})^2} \left[- \frac{2 [t_2^\dagger t_2^{\dagger}]^{\mu\nu} [t_1^\dagger t_1^\dagger]^{\alpha\beta}}{2U_f^+ + U_p + 2\Delta_{pf}} + \left(\frac{1}{U_f^+ + U_f^-} + \frac{2}{2U_f^+ + U_p + 2\Delta_{pf}} \right) [t_2^\dagger t_1^\dagger]^{\mu\beta} [t_1^\dagger t_2^\dagger]^{\alpha\nu} \right]. \quad (12)$$

Here we dropped constants and single site terms that serve only to renormalize the on-site single-ion Hamiltonian.

Generically, the interactions \mathcal{I} are complicated due to the f^9 states that make up the ${}^6\text{H}_{15/2}$ ground state manifold of Dy^{3+} . However, a strong constraint arises from the one-electron form $f_\alpha^\dagger f_\beta$ taken by the operators at each rare-earth site. When projected into the ${}^6\text{H}_{15/2}$ manifold, these operators can generate only a small subset of all possible interactions between the $J = 15/2$ degrees of freedom of Dy^{3+} . This can be seen explicitly by considering how these operators transform under rotations. Since each f electron carries a total angular momentum of $J = 5/2$ or $J = 7/2$, the operators $f_\alpha^\dagger f_\beta$ are multipoles with rank ranging from rank-0 ($5/2 - 5/2$ or $7/2 - 7/2$) up to rank-7 ($7/2 + 7/2$). Hence, we find that *only multipolar interactions up to rank-7 are generated by super-exchange*. Because of the spherical symmetry of the free ions; the complicated intra-atomic interactions are rank-0 operators and thus *do not* change the rank counting above [41].

Including the CEF splittings in the resolvents only changes this result slightly. Given the small overall splitting $\Delta \lesssim 100 \text{ meV}$ induced by the CEF [30, 42], we can treat this as a perturbation to H_0 along with V . Since the CEF potential is a one-electron operator and is time-reversal invariant, it contains only operators up to rank-6 for the same reasons as discussed above [50]. Each inclusion of the CEF operator can thus increase the rank by 6, with up to rank-13 operators at order $\sim \Delta/U_f^\pm$, and operators up to the maximal rank-15 at order $\sim (\Delta/U_f^\pm)^2$. The rank-15 operators that directly link the leading $|\pm 15/2\rangle$ components are thus *strongly suppressed* by a factor of $(\Delta/U_f^\pm)^2 \sim 10^{-4}$. We can thus ignore these small corrections and can consider only interactions of rank-7 or lower.

General argument: Returning to a more general physical picture, the above results allow us to explain why quantum effects are small in the classical spin ices $\text{Dy}_2\text{Ti}_2\text{O}_7$ and

$\text{Ho}_2\text{Ti}_2\text{O}_7$. Given the dominant $|\pm 15/2\rangle$ or $|\pm 8\rangle$ CEF ground states in Dy^{3+} and Ho^{3+} [30], a large transverse scale J_{\pm} must originate from *very* high-rank multipole interactions. These multipole interactions are only generated weakly from super-exchange contributions, as they are much higher than rank-7. Due to this suppression, the leading contributions to the transverse couplings must come from the sub-dominant spectral components of the CEF ground doublet, the δ_n components given in Eq. (1) for $\text{Dy}_2\text{Ti}_2\text{O}_7$. When these are included, generation of J_{\pm} by super-exchange becomes feasible. As a rough estimate, if J is the typical scale of contributions from super-exchange then we expect

$$J_{\pm} \sim \left(\frac{\delta}{\alpha}\right)^2 J, \quad J_z \sim -J, \quad (13)$$

where δ represents the maximum size of the sub-dominant components of the CEF doublet. Each transverse pseudo-spin operator S^{\pm} contributes one factor of δ/α to the scale J_{\pm} [51]. Since we can constrain $\delta/\alpha \lesssim 0.1$ via the size of the magnetic moment, then one expects, all things being equal, the transverse scale J_{\pm} to be suppressed by two orders of magnitude relative to the super-exchange contributions to the Ising coupling J_z . Since we know $J \sim 5$ K in $\text{Dy}_2\text{Ti}_2\text{O}_7$ [13, 16] and $J \sim 2$ K in $\text{Ho}_2\text{Ti}_2\text{O}_7$ [15], this implies $J_{\pm} \lesssim 50$ mK. This is the main conclusion of our work.

Estimate from model calculation: The simple scaling argument above does not include combinatoric factors or other unforeseen quirks or cancellations that could favor or disfavor the generation of transverse J_{\pm} couplings. To check that such anomalies do not occur, we carry out an explicit calculation to verify this scaling estimate. We work within the charging approximation as encapsulated in Eq. (12), considering only a single super-exchange path.

The shortest path between the rare-earth ions and oxygen passes through the O' site situated in the center of each tetrahedron. Within the Slater-Koster approximation [52], the hopping matrices t_1, t_2 can be expressed as $t_i = R_i^{\dagger} t_0$ where R_i is a rotation of the f and p orbitals that takes a set of axes aligned to the i local axes into the global frame. The matrices t_0 define overlaps in the frame aligned along the bond axis and take the simple form $[t_0]_{mm'} = \delta_{mm'}(\delta_{|m|=1} t_{pf\pi} + \delta_{m=0} t_{pf\sigma})$. We note that $t_{pf\pi}$ is smaller in magnitude than $t_{pf\sigma}$ and of opposite sign [53], though their precise values will not be important to our discussion. Since t_0 is diagonal and R_i is unitary, the products that appear in Eq. (12) are

$$[t_i t_j^{\dagger}]^{\alpha\beta} = t_0^{\alpha} t_0^{\beta} [R_i^{\dagger} R_j]^{\alpha\beta}, \quad [t_i t_i^{\dagger}]^{\alpha\beta} = (t_0^{\alpha})^2 \delta_{\alpha\beta}, \quad (14)$$

as in Ref. [34]. Consideration of further super-exchange paths between the other oxygen atoms would change the form of t_i , but not the overall structure of the interactions.

To evaluate the super-exchange interactions, we proceed as follows: we first construct the CEF ground doublet states of Eq. (1) from the full f^9 manifold. Next, we project the one-electron operators $f_{\alpha}^{\dagger} f_{\beta}$ into this basis. Finally we sum these one-electron operators with the interaction constants of Eq.

(12) evaluated using the t_i given above for single bond of the lattice. The remaining bonds can be recovered using the lattice symmetry. This gives a model of the form shown in Eq. (5). At leading order in the δ_n coefficients, one has

$$J_{xx} = -4J \left(\frac{\delta_5}{\alpha}\right)^2 + O(\alpha\delta^3), \quad J_{xz} = +2J \left(\frac{\delta_5}{\alpha}\right) + O(\alpha\delta^2), \\ J_{zz} = -J + O(\alpha\delta^2), \quad J_{yy} = 0 + O(\alpha\delta^3), \quad (15)$$

where all of the δ_n have been considered at the same order in the expansion [54]. The super-exchange energy scale J is

$$J = \frac{2\alpha^4 t_{pf\sigma}^4}{(U_f^+ + \Delta)^2} \left(\frac{1}{U_f^+ + U_f^-} + \frac{2}{2U_f^+ + U_p + 2\Delta} \right) \times \\ \frac{1}{2187} \left(121 + 96 \left(\frac{t_{pf\pi}}{t_{pf\sigma}}\right)^2 + 450 \left(\frac{t_{pf\pi}}{t_{pf\sigma}}\right)^4 \right). \quad (16)$$

From Eqs. (15) and (16), we see that our naïve scaling argument of $J_{\pm} \sim (\delta/\alpha)^2 J$ does in fact hold in this more detailed calculation. We also note that the sign of the super-exchange contribution to J_{zz} is negative, as required for $\text{Dy}_2\text{Ti}_2\text{O}_7$ [13, 16].

Only the super-exchange contribution to J_{zz} has been computed here; when rotating to eliminate the J_{xz} coupling, we must also include the large contribution D to J_{zz} coming from the nearest-neighbor part of the MDD interactions. We thus shift $J_{zz} \rightarrow J_{zz} + D$ where D is given in Eq. (8). Using the approximate rotations of Eq. (7), we find $J_y \sim 0$ and

$$J_x = -\frac{4DJ}{D-J} \left(\frac{\delta_5}{\alpha}\right)^2, \quad J_z = D - J + \frac{4J^2}{D-J} \left(\frac{\delta_5}{\alpha}\right)^2. \quad (17)$$

From the constraint on the moment size, we find $\delta_5^2/\alpha^2 \leq 0.005$ so then $J_{\pm} \lesssim 56$ mK. At the temperature scale of interest, monopole excitations [10] are suppressed and quantum effects can proceed only through quantum tunnelling *within* the spin ice manifold [55]. The strength of tunnelling g appears perturbatively at third-order in the transverse coupling as $g \sim 12J_{\pm}^3/J_z^2$ [43, 55, 56]. Using the above estimate, these quantum effects would only become relevant for temperatures $\lesssim 0.14$ mK in $\text{Dy}_2\text{Ti}_2\text{O}_7$. In fact, this estimate could be reduced significantly depending on how close the sub-leading spectral components of $|\pm\rangle$ are to their maximal values allowed by the moment size. For example, using the CEF parameters of Bertin *et al.* [42], one has $\delta_5 \sim 10^{-3}$ which is much smaller than the bound implied by $\delta_n^2 \lesssim 0.025/n$ from the moment, giving a significantly smaller transverse coupling J_{\pm} . Following the same methods, the estimate for tunnelling in $\text{Ho}_2\text{Ti}_2\text{O}_7$ is also $\lesssim 0.1$ mK [41].

Outlook: We have presented a general argument as to why transverse exchanges in the canonical spin ices are small. In particular, we have shown that the generation of the required high rank multipolar couplings needed to link the nearly maximal $|\pm\rangle$ states of the CEF doublets are strongly suppressed. Using an approximate treatment of the oxygen mediated super-exchange interaction, we have provided some

heuristic bounds on this size of these couplings. The presence of all these factors can provide an explanation of spin ice behavior in the related germanates $\text{Ho}_2\text{Ge}_2\text{O}_7$ [32, 39] and $\text{Dy}_2\text{Ge}_2\text{O}_7$ [29, 39] or the stannates $\text{Ho}_2\text{Sn}_2\text{O}_7$ [28, 37] and $\text{Dy}_2\text{Sn}_2\text{O}_7$ [28, 38]. These criteria also suggest what features to look for to move away from the classical spin ice limit [5]. For example, compounds with Kramers ions and large Ising-like moments, but significant sub-leading components in their ground state CEF doublet could present quantum behavior at more experimentally relevant temperature scales [5]. In this context, the spinel CdEr_2Se_4 [57] with Ising Er^{3+} moment is an intriguing example where this logic may apply.

Acknowledgements: We thank Zhihao Hao for useful discussions. This work was supported by the NSERC of Canada, the Canada Research Chair program (M. J. P. G., Tier 1), the Canadian Foundation for Advanced Research and the Perimeter Institute (PI) for Theoretical Physics. Research at PI is supported by the Government of Canada through Industry Canada and by the Province of Ontario through the Ministry of Economic Development & Innovation. M.G. acknowledges the hospitality and generous support of the Quantum Matter Institute at the University of British Columbia and TRIUMF where part of this work was completed.

Note added: After completion of this work, a preprint appeared, Ref. [58], that reaches some similar conclusions on the interactions between $^{2S+1}L_J$ multiplets in rare-earth ions.

-
- [1] S. T. Bramwell and M. J. P. Gingras, “Spin ice state in frustrated magnetic pyrochlore materials,” *Science* **294**, 1495 (2001).
- [2] M. J. P. Gingras, “Spin ice,” in *Highly Frustrated Magnetism*, Springer Series in Solid-State Sciences, Vol. 164, edited by C Lacroix, P Mendels, and F Mila (Springer, 2011).
- [3] J. S. Gardner, M. J. P. Gingras, and J. E. Greedan, “Magnetic pyrochlore oxides,” *Rev. Mod. Phys.* **82**, 53 (2010).
- [4] C. Castelnovo, R. Moessner, and S. L. Sondhi, “Spin ice, fractionalization, and topological order,” *Annual Review of Condensed Matter Physics* **3**, 35–55 (2012).
- [5] M. J. P. Gingras and P. A. McClarty, “Quantum spin ice: a search for gapless quantum spin liquids in pyrochlore magnets,” *Rep. Prog. Phys.* **77**, 056501 (2014).
- [6] J. Villain, “Insulating spin glasses,” *Z. für Physik B* **33**, 31 (1979).
- [7] M. J. Harris, S. T. Bramwell, D. F. McMorrow, T. Zeiske, and K. W. Godfrey, “Geometrical frustration in the ferromagnetic pyrochlore $\text{Ho}_2\text{Ti}_2\text{O}_7$,” *Phys. Rev. Lett.* **79**, 2554 (1997).
- [8] A. P. Ramirez, A. Hayashi, R. J. Cava, R. Siddharthan, and B. S. Shastry, “Zero-point entropy in spin ice,” *Nature* **399**, 333 (1999).
- [9] A. L. Cornelius and J. S. Gardner, “Short-range magnetic interactions in the spin-ice compound $\text{Ho}_2\text{Ti}_2\text{O}_7$,” *Phys. Rev. B* **64**, 060406 (2001).
- [10] C. Castelnovo, R. Moessner, and S. L. Sondhi, “Magnetic monopoles in spin ice,” *Nature* **451**, 42 (2008).
- [11] C. L. Henley, “The ‘Coulomb Phase’ in frustrated systems,” *Annual Review of Condensed Matter Physics* **1**, 179 (2010).
- [12] S. V. Isakov, K. Gregor, R. Moessner, and S. L. Sondhi, “Dipolar spin correlations in classical pyrochlore magnets,” *Phys. Rev. Lett.* **93**, 167204 (2004).
- [13] B. C. den Hertog and M. J. P. Gingras, “Dipolar interactions and origin of spin ice in Ising pyrochlore magnets,” *Phys. Rev. Lett.* **84**, 3430 (2000).
- [14] J. P. C. Ruff, R. G. Melko, and M. J. P. Gingras, “Finite-temperature transitions in dipolar spin ice in a large magnetic field,” *Phys. Rev. Lett.* **95**, 097202 (2005).
- [15] S. T. Bramwell, M. J. Harris, B. C. den Hertog, M. J. P. Gingras, J. S. Gardner, D. F. McMorrow, A. R. Wildes, A. L. Cornelius, J. D. M. Champion, R. G. Melko, *et al.*, “Spin correlations in $\text{Ho}_2\text{Ti}_2\text{O}_7$: a dipolar spin ice system,” *Phys. Rev. Lett.* **87**, 047205 (2001).
- [16] T. Yavors’kii, T. Fennell, M. J. P. Gingras, and S. T. Bramwell, “ $\text{Dy}_2\text{Ti}_2\text{O}_7$ spin ice: a test case for emergent clusters in a frustrated magnet,” *Phys. Rev. Lett.* **101**, 037204 (2008).
- [17] Y. Tabata, H. Kadowaki, K. Matsuura, Z. Hiroi, N. Aso, E. Ressouche, and B. Fåk, “Kagome ice state in the dipolar spin ice $\text{Dy}_2\text{Ti}_2\text{O}_7$,” *Phys. Rev. Lett.* **97**, 257205 (2006).
- [18] M. J. P. Gingras and B. C. den Hertog, “Origin of spin-ice behavior in Ising pyrochlore magnets with long-range dipole interactions: an insight from mean-field theory,” *Can. J. Phys.* **79**, 1339 (2001).
- [19] R. G. Melko, B. C. den Hertog, and M. J. P. Gingras, “Long-range order at low temperatures in dipolar spin ice,” *Phys. Rev. Lett.* **87**, 067203 (2001).
- [20] R. G. Melko and M. J. P. Gingras, “Monte carlo studies of the dipolar spin ice model,” *J. Phys. Condens. Matter* **16**, R1277 (2004).
- [21] S. V. Isakov, R. Moessner, and S. L. Sondhi, “Why spin ice obeys the ice rules,” *Phys. Rev. Lett.* **95**, 217201 (2005).
- [22] H. Fukazawa, R. G. Melko, R. Higashinaka, Y. Maeno, and M. J. P. Gingras, “Magnetic anisotropy of the spin-ice compound $\text{Dy}_2\text{Ti}_2\text{O}_7$,” *Phys. Rev. B* **65**, 054410 (2002).
- [23] D. Pomaranski, L. R. Yaraskavitch, S. Meng, K. A. Ross, H. M. L. Noad, H. A. Dabkowska, B. D. Gaulin, and J. B. Kycia, “Absence of Pauling’s residual entropy in thermally equilibrated $\text{Dy}_2\text{Ti}_2\text{O}_7$,” *Nat. Phys.* **9**, 353 (2013).
- [24] N. Shannon, “Magnetic monopoles: Entropy lost,” *Nature Physics* **9**, 326 (2013).
- [25] P. McClarty, O. Sikora, R. Moessner, K. Penc, F. Pollmann, and N. Shannon, “What is the quantum ground state of dipolar spin ice?” (2014), [arXiv:1410.0451 \[cond-mat\]](https://arxiv.org/abs/1410.0451).
- [26] R. Siddharthan, B. S. Shastry, A. P. Ramirez, and A. Hayashi, “Ising pyrochlore magnets: low-temperature properties, ‘ice rules’, and beyond,” *Phys. Rev. Lett.* **83**, 1854 (1999).
- [27] D. J. Flood, “Magnetization and magnetic entropy of $\text{Dy}_2\text{Ti}_2\text{O}_7$,” *J. Appl. Phys.* **45**, 4041 (1974).
- [28] K. Matsuura, Y. Hinatsu, K. Tenya, H. Amitsuka, and T. Sakakibara, “Low-temperature magnetic properties of pyrochlore stannates,” *Journal of the Physical Society of Japan* **71**, 1576 (2002).
- [29] X. Ke, M. L. Dahlberg, E. Morosan, J. A. Fleitman, R. J. Cava, and P. Schiffer, “Magnetothermodynamics of the Ising antiferromagnet $\text{Dy}_2\text{Ge}_2\text{O}_7$,” *Phys. Rev. B* **78**, 104411 (2008).
- [30] S. Rosenkranz, A. P. Ramirez, A. Hayashi, R. J. Cava, R. Siddharthan, and B. S. Shastry, “Crystal-field interaction in the pyrochlore magnet $\text{Ho}_2\text{Ti}_2\text{O}_7$,” *J. Appl. Phys.* **87**, 5914 (2000).
- [31] O. A. Petrenko, M. R. Lees, and G. Balakrishnan, “Magnetization process in the spin-ice compound $\text{Ho}_2\text{Ti}_2\text{O}_7$,” *Phys. Rev. B* **68**, 012406 (2003).
- [32] A. M. Hallas, J. A. M. Paddison, H. J. Silverstein, A. L. Goodwin, J. R. Stewart, A. R. Wildes, J. G. Cheng, J. S. Zhou, J. B. Goodenough, E. S. Choi, G. Ehlers, J. S. Gardner, C. R. Wiebe, and H. D. Zhou, “Statics and dynamics of the highly correlated

- spin ice $\text{Ho}_2\text{Ge}_2\text{O}_7$,” *Phys. Rev. B* **86**, 134431 (2012).
- [33] P. Santini, S. Carretta, G. Amoretti, R. Caciuffo, N. Magnani, and G. H. Lander, “Multipolar interactions in f-electron systems: The paradigm of actinide dioxides,” *Rev. Mod. Phys.* **81**, 807 (2009).
- [34] S. Onoda and Y. Tanaka, “Quantum fluctuations in the effective pseudospin- $\frac{1}{2}$ model for magnetic pyrochlore oxides,” *Phys. Rev. B* **83**, 094411 (2011).
- [35] H. D. Zhou, C. R. Wiebe, J. A. Janik, L. Balicas, Y. J. Yo, Y. Qiu, J. R. D. Copley, and J. S. Gardner, “Dynamic spin ice: $\text{Pr}_2\text{Sn}_2\text{O}_7$,” *Phys. Rev. Lett.* **101**, 227204 (2008).
- [36] K. Kimura, S. Nakatsuji, J. J. Wen, C. Broholm, M. B. Stone, E. Nishibori, and H. Sawa, “Quantum fluctuations in spin-ice-like $\text{Pr}_2\text{Zr}_2\text{O}_7$,” *Nat. Comm.* **4**, 1934 (2013).
- [37] H. Kadowaki, Y. Ishii, K. Matsuhira, and Y. Hinatsu, “Neutron scattering study of dipolar spin ice $\text{Ho}_2\text{Sn}_2\text{O}_7$: frustrated pyrochlore magnet,” *Phys. Rev. B* **65**, 144421 (2002).
- [38] K. Matsuhira, M. Wakeshima, Y. Hinatsu, C. Sekine, C. Paulsen, T. Sakakibara, and S. Takagi, “Slow dynamics of Dy pyrochlore oxides $\text{Dy}_2\text{Sn}_2\text{O}_7$ and $\text{Dy}_2\text{Ir}_2\text{O}_7$,” *J. Phys.: Conf. Ser.* **320**, 012050 (2011).
- [39] H. D. Zhou, J. G. Cheng, A. M. Hallas, C. R. Wiebe, G. Li, L. Balicas, J. S. Zhou, J. B. Goodenough, J. S. Gardner, and E. S. Choi, “Chemical pressure effects on pyrochlore spin ice,” *Phys. Rev. Lett.* **108**, 207206 (2012).
- [40] While not explicitly stated in the literature, this result is implicit in many earlier works on super-exchange in rare-earths, see for example Refs. [33, 34, and 59]. Very recent work by Iwahara and Chibotaru [58] has also explicitly pointed this out.
- [41] See Supplemental Material at [] for an argument on quantum effects in $\text{Ho}_2\text{Ti}_2\text{O}_7$, a more detailed discussion of super-exchange and the suppression of high-rank multipoles, and an outline of other possible sources of microscopic interactions among the rare-earth angular momenta.
- [42] A. Bertin, Y. Chapuis, P. Dalmas de Réotier, and A. Yaouanc, “Crystal electric field in the $\text{R}_2\text{Ti}_2\text{O}_7$ pyrochlore compounds,” *J. Phys. Condens. Matter* **24**, 256003 (2012).
- [43] Y. Huang, G. Chen, and M. Hermele, “Quantum spin ices and topological phases from dipolar-octupolar doublets on the pyrochlore lattice,” *Phys. Rev. Lett.* **112**, 167203 (2014).
- [44] E. U. Condon and G. H. Shortley, *The theory of atomic spectra* (Cambridge University Press, 1951).
- [45] H. R. Molavian, M. J. P. Gingras, and B. Canals, “Dynamically induced frustration as a route to a quantum spin ice state in $\text{Tb}_2\text{Ti}_2\text{O}_7$ via virtual crystal field excitations and quantum many-body effects,” *Phys. Rev. Lett.* **98**, 157204 (2007).
- [46] Note that some prior work uses a different convention for their Ising variables, taking values ± 1 rather than the pseudo-spin $\pm 1/2$ used here. This accounts for a factor of four difference in the stated exchange constants D and J .
- [47] The sign convention for J is reversed relative to some prior work in Refs. [13, 14, 19, 20].
- [48] I. Lindgren, “The Rayleigh-Schrodinger perturbation and the linked-diagram theorem for a multi-configurational model space,” *J. Phys. B: At. Mol.* **7**, 2441 (1974).
- [49] D. Van der Marel and G. A. Sawatzky, “Electron-electron interaction and localization in d and f transition metals,” *Phys. Rev. B* **37**, 10674 (1988).
- [50] K. W. H. Stevens, “Matrix elements and operator equivalents connected with the magnetic properties of rare earth ions,” *Proc. Phys. Soc. A* **65**, 209 (1952).
- [51] For the case of the $\Gamma_5 \oplus \Gamma_6$ doublet of $\text{Dy}_2\text{Ti}_2\text{O}_7$, the J_{xz} exchange will be of order δ/α , since only one of the pseudo-spins is transverse. Redefining the axes by the rotation (7), we recover the estimate as stated.
- [52] J. C. Slater and G. F. Koster, “Simplified LCAO method for the periodic potential problem,” *Phys. Rev.* **94**, 1498 (1954).
- [53] K. Takegahara, Y. Aoki, and A. Yanase, “Slater-Koster tables for f electrons,” *J. Phys. C: Solid State Phys.* **13**, 583 (1980).
- [54] To perform this expansion we treat all δ_n as equally small. Practically speaking, we replace $\delta_n \rightarrow \eta\delta_n$ and expand to leading order in η , then send $\eta \rightarrow 1$. Statements such as $O(\delta^2)$ imply the dropped terms involve a product of some pair of the δ_n .
- [55] M. Hermele, M. P. A. Fisher, and L. Balents, “Pyrochlore photons: The U(1) spin liquid in a $S = 1/2$ three-dimensional frustrated magnet,” *Phys. Rev. B* **69**, 064404 (2004).
- [56] Y. Kato and S. Onoda, “Numerical evidence of quantum melting of spin ice: quantum-classical crossover,” (2014), [arXiv:1411.1918 \[cond-mat\]](https://arxiv.org/abs/1411.1918).
- [57] J. Lago, I. Živković, B. Z. Malkin, J. Rodriguez Fernandez, P. Ghigna, P. Dalmas de Réotier, A. Yaouanc, and T. Rojo, “ CdEr_2Se_4 : A new erbium spin ice system in a spinel structure,” *Phys. Rev. Lett.* **104**, 247203 (2010).
- [58] N. Iwahara and L. F. Chibotaru, “Exchange interaction between J -multiplets,” (2015), [arXiv:1503.02462 \[cond-mat\]](https://arxiv.org/abs/1503.02462).
- [59] R. J. Elliott and M. F. Thorpe, “Orbital effects on exchange interactions,” *J. Appl. Phys.* **39**, 802 (1968).

Supplemental Material for “How quantum are classical spin ices?”

Jeffrey G. Rau¹ and Michel J. P. Gingras^{1,2,3}

¹*Department of Physics and Astronomy,
University of Waterloo, Ontario, N2L 3G1, Canada*

²*Perimeter Institute for Theoretical Physics,
Waterloo, Ontario, N2L 2Y5, Canada*

³*Canadian Institute for Advanced Research, 180 Dundas Street West,
Suite 1400, Toronto, ON, M5G 1Z8, Canada*

TRANSVERSE INTERACTIONS IN HOLMIUM TITANATE

Ground state doublet

In the case of Ho^{3+} , the crystal field (CEF) ground state is a non-Kramers doublet built from the $^5\text{I}_8$ manifold of the $4f^{10}$ configuration [1, 2]. The first excited CEF level is ~ 20 meV above the ground doublet [2]. This non-Kramers doublet transforms in the E_g representation of the D_{3d} site symmetry group and can be written

$$|\pm\rangle = \alpha |\pm 8\rangle \mp \delta_1 |\pm 5\rangle + \delta_2 |\pm 2\rangle \mp \delta_3 |\mp 1\rangle + \delta_4 |\mp 4\rangle \mp \delta_5 |\mp 7\rangle \quad (1)$$

where $|M\rangle \equiv |8, M\rangle$ are eigenstates of the J^2 and J^z operators of the $^5\text{I}_8$ manifold. This doublet is naturally Ising-like with

$$\langle \sigma | J^\pm | \sigma' \rangle = 0, \quad \langle \sigma | J^z | \sigma' \rangle = \lambda \sigma \delta_{\sigma\sigma'}, \quad (2)$$

where $\sigma = \pm$ and the λ -factor is

$$\lambda \equiv 8 - 3(\delta_1^2 + 2\delta_2^2 + 3\delta_3^2 + 4\delta_4^2 + 5\delta_5^2). \quad (3)$$

Including the Ho^{3+} Landé factor, $g = 5/4$, the magnetic moment $\mu = g\mu_B\lambda$ is found to be very close to the maximal $10\mu_B$ experimentally [1, 3, 4]. This constrains the spectral content of the $|\pm\rangle$ states in Eq. (1) to be predominantly $|\pm 8\rangle$. We can also appeal to more detailed information on the CEF structure. Fits to the CEF levels obtained via neutron scattering have yielded estimates of the sub-leading components δ_n . For example, work by Bertin *et al.* [5] gives

$$\delta_1 = 0.189, \quad \delta_2 = 0.014, \quad \delta_3 = 0.070, \quad \delta_4 = 0.031, \quad \delta_5 = 0.005. \quad (4)$$

Rather than rely on these parameters, we shall consider the bound implied by a deviation of the moment from maximal by some amount ϵ . In $\text{Dy}_2\text{Ti}_2\text{O}_7$, we used $\epsilon = 0.01$ due to the $\pm 0.1\mu_B$ error bar from Ref. [6]. For $\text{Ho}_2\text{Ti}_2\text{O}_7$ this relation is $\delta_n^2 \lesssim 8\epsilon/(3n)$, but given the lack of stated bound on the moment, we use a more conservative $\epsilon = 0.05$ which implies $\delta_n^2 \lesssim 0.133/n$.

Effective pseudo-spin 1/2 model

We proceed similarly to the $\text{Dy}_2\text{Ti}_2\text{O}_7$ case in the main text. Since the CEF energy scale is large, it is sufficient to first consider only a bare projection of the microscopic Ho^{3+} - Ho^{3+} interactions

acting within the full 5I_8 manifold into the ground doublets. Such a model can be expressed in terms of the pseudo-spin 1/2 operators

$$S^\pm = |\pm\rangle\langle\mp|, \quad S^z = \frac{1}{2}(|+\rangle\langle+| - |-\rangle\langle-|). \quad (5)$$

acting within the low-energy Hilbert space spanned by the $|\pm\rangle$ doublets. The symmetry of pyrochlore lattice constrains the form of any such projected Hamiltonian. For a non-Kramers doublet, a nearest-neighbor model can be shown to be restricted to the form [7, 8]

$$\sum_{\langle ij \rangle} \left[J_{zz} S_i^z S_j^z - J_\pm (S_i^+ S_j^- + S_i^- S_j^+) + J_{\pm\pm} (\gamma_{ij} S_i^+ S_j^+ + \gamma_{ij}^* S_i^- S_j^-) \right]. \quad (6)$$

where the bond dependent phases γ_{ij} are defined in Ref. [8]. Once dipolar interactions are included, we will find that J_{zz} is the dominant bare coupling and that it is positive. We will characterize deviations from the Ising limit using the nearest-neighbor transverse scale J_\pm , as quantum effects from $J_{\pm\pm}$ appear at higher order in perturbation theory [8, 9]. Our goal is to estimate the size of J_\pm which is responsible for the quantum dynamics within the low-energy pseudo-spin 1/2 model.

Ising interactions

As in $\text{Dy}_2\text{Ti}_2\text{O}_7$, the long-range dipole-dipole interactions play an important role, In $\text{Ho}_2\text{Ti}_2\text{O}_7$ these take the same form

$$\mathcal{D} \sum_{ij} S_i^z S_j^z \left(\frac{r_{ij}}{r_m} \right)^3 \left[\hat{z}_i \cdot \hat{z}_j - (\hat{r}_{ij} \cdot \hat{z}_i)(\hat{r}_{ij} \cdot \hat{z}_j) \right], \quad (7)$$

where r_m is the nearest-neighbor distance between the rare-earth atoms, $\vec{r}_{ij} \equiv \vec{r}_i - \vec{r}_j$ is the displacement vector between the two sites and \hat{z}_i is the quantization axis along the local cubic [111] direction at site \vec{r}_i . The strength of the coupling is characterized by $\mathcal{D} = g^2 \lambda^2 \mu_B^2 \mu_0 / (4\pi r_m^3)$. The largest piece is the nearest-neighbor contribution, with coefficient $D \equiv 5\mathcal{D}/3$ which is ~ 9.4 K in $\text{Ho}_2\text{Ti}_2\text{O}_7$ [10], slightly larger than in $\text{Dy}_2\text{Ti}_2\text{O}_7$. As in $\text{Dy}_2\text{Ti}_2\text{O}_7$, to obtain a quantitative agreement with experiments, corrections to the Ising couplings must be included. The nearest-neighbor correction J is the largest, estimated to be ~ 2.08 K [11] for $\text{Ho}_2\text{Ti}_2\text{O}_7$.

Model calculation

We follow the same procedure as in the main text for $\text{Dy}_2\text{Ti}_2\text{O}_7$, this time working with the states defined in Eq. (1) drawn from the $4f^{10}$ manifold appropriate for Ho^{3+} . Aside from the

construction of these states, the methods are identical. We find

$$J_{\pm} = +J \cdot \rho_{\pm} \left(\frac{t_{pf\pi}}{t_{pf\sigma}} \right) \left(\frac{\delta_5}{\alpha} \right)^2 + O(\alpha\delta^3), \quad (8a)$$

$$J_{\pm\pm} = -J \cdot \rho_{\pm\pm} \left(\frac{t_{pf\pi}}{t_{pf\sigma}} \right) \left(\frac{\delta_5}{\alpha} \right)^2 + O(\alpha\delta^3), \quad (8b)$$

$$J_{zz} = -J + O(\alpha^3\delta), \quad (8c)$$

where all of the δ_n have been considered at the same order in the expansion. The super-exchange energy scale J is given by

$$J = \frac{4\alpha^4 t_{pf\sigma}^4}{(U_f^+ + \Delta_{pf})^2} \left(\frac{1}{U_f^+ + U_f^-} + \frac{2}{2U_f^+ + U_p + 2\Delta_{pf}} \right) \frac{1}{2187} \left(121 + 48 \left(\frac{t_{pf\pi}}{t_{pf\sigma}} \right)^2 + 207 \left(\frac{t_{pf\pi}}{t_{pf\sigma}} \right)^4 \right). \quad (9)$$

The ρ_{\pm} and $\rho_{\pm\pm}$ are rational functions of the ratio $x \equiv t_{pf\pi}/t_{pf\sigma}$ defined as

$$\rho_{\pm}(x) = \frac{9x^2(160 - 8x + 7x^2)}{8(121 + 48x^2 + 207x^4)}, \quad \rho_{\pm\pm}(x) = \frac{9x^2(68 - 16x - 7x^2)}{16(121 + 48x^2 + 207x^4)}. \quad (10)$$

Reasonable values of the Slater-Koster ratio satisfy $-1 < t_{pf\pi}/t_{pf\sigma} < 0$. For this range, we can bound these functions as

$$0 < \rho_{\pm}(t_{pf\pi}/t_{pf\sigma}) \lesssim 0.6, \quad 0 < \rho_{\pm\pm}(t_{pf\pi}/t_{pf\sigma}) \lesssim 0.15. \quad (11)$$

As in $\text{Dy}_2\text{Ti}_2\text{O}_7$, we see that scaling from the main text, $J_{\pm} \sim (\delta/\alpha)^2 J$ holds with no large combinatoric factors or spurious cancellations. We also note that the sign of the super-exchange contribution to the J_{zz} is again, correctly negative [10]. Setting the super-exchange scale to $J = 2.08$ K from the experimental constraints [10], we then can estimate J_{\pm} and $J_{\pm\pm}$ as

$$J_{\pm} \lesssim 1.25 \text{ K} \cdot \left(\frac{\delta_5}{\alpha} \right)^2, \quad |J_{\pm\pm}| \lesssim 0.31 \text{ K} \cdot \left(\frac{\delta_5}{\alpha} \right)^2. \quad (12)$$

For a moment size that deviates from maximal by $\epsilon = 0.05$, this ratio is bounded as $(\delta_5/\alpha)^2 \lesssim 0.027$ giving

$$J_{\pm} \lesssim 34 \text{ mK}, \quad |J_{\pm\pm}| \lesssim 8.5 \text{ mK}. \quad (13)$$

Here the relevant transverse scale is the J_{\pm} that appears in the nearest-neighbor model (6). With $J_z = D - J \sim 7.32$ K, the implied tunnelling scale g is $\ll 0.1$ mK and thus is not experimentally relevant. We note that these estimates for J_{\pm} and $J_{\pm\pm}$ scale linearly in the deviation from the maximal moment. For the CEF parameters of Ref. [5] we have $(\delta_5/\alpha)^2 \sim 10^{-6}$, and one would have to look at next order in the δ_n to get at the true leading behavior. It is unclear if the fitting of the CEF energy levels is sufficiently precise to provide a useful estimate of the true size of δ_5 .

GENERAL DISCUSSION OF SUPER-EXCHANGE

We use the notation of the main text. As discussed there, we consider the bare Hamiltonian of the two rare-earth sites and the intermediate oxygen atom

$$H_0 \equiv H_{f,1} + H_{f,2} + H_p. \quad (14)$$

We perturb this with the hybridization terms

$$V \equiv \sum_{\alpha\beta} \left[t_{1,\alpha\beta}^\dagger p_\alpha^\dagger f_{1\beta} + t_{1,\alpha\beta} f_{1\alpha}^\dagger p_\beta + t_{2,\alpha\beta}^\dagger p_\alpha^\dagger f_{2\beta} + t_{2,\alpha\beta} f_{2\alpha}^\dagger p_\beta \right], \quad (15)$$

Exchange interactions between the rare-earth ions come in at fourth-order in V . We will follow Lindgren [12] and write the effective Hamiltonian using the ground state projector P and resolvent operator R

$$P = \sum_{\alpha \in 0} |\alpha\rangle \langle \alpha|, \quad R = \sum_{a \neq 0} \frac{|\alpha\rangle \langle a|}{E_0 - E_a}, \quad (16)$$

where $|\alpha\rangle$ are ground states of H_0 with energy E_0 and $|a\rangle$ are the excited states of H_0 with energies E_a . The fourth-order effective Hamiltonian is then [12]

$$\begin{aligned} H_{\text{eff}} = & PVRVRVRVP - PVR^2VPVRVP - PVR^2VRVPVP \\ & - PVRVR^2VPVP + PVR^2VPVPVP \end{aligned} \quad (17)$$

Now since $PVP = 0$, we can drop all but the two terms $PVRVRVRVP$ and $PVR^2VPVRVP$. The second of these factors as $(PVR^2VP)(PVRVP)$ and serves to cancel non-extensive contributions that arise from the first term.

We thus can simply use $H_{\text{eff}} \sim PVRVRVRVP$, taking to care to consider only this set of (extensive) perturbative processes. At lowest order, we need only consider the excited configurations that can be built by moving at most two electrons between the rare-earth and oxygen sites. These types of intermediate states can be understood by considering the possible values for the oxygen electron number. The range of accessible states are illustrated in Figures 1, 2 and 3. Starting from the ground state $f^n p^6 f^n$ configuration, one follows the colored arrows to trace out a given exchange path. Spin and orbital indices on the f and p electron operators have been suppressed for clarity. We see only two distinct types of processes are needed at fourth order, process 1 (Figure 1) which creates at most one hole on the oxygen and processes 2 and 3 (Figure 2 and Figure 3) which create an intermediate state with two holes on the oxygen. A second set of equivalent paths

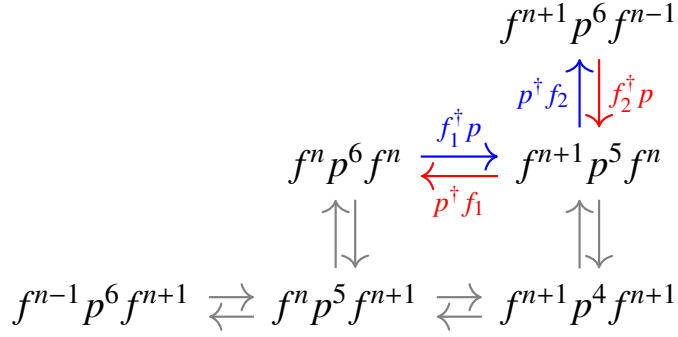


FIG. 1: Process 1 involves intermediate states with only a single hole on the oxygen site. Scales roughly as $\sim t^4(U_f + \Delta_{pf})^{-2}(2U_f)^{-1}$

can be obtained by switching the role of sites 1 and 2 in the processes. Process 1 corresponds to the pieces of H_{eff} of the form

$$P \left[p^\dagger t_1^\dagger f_1 \right] R \left[f_2^\dagger t_2 p \right] R \left[p^\dagger t_2^\dagger f_2 \right] R \left[f_1^\dagger t_1 p \right] P. \quad (18)$$

Each appearance of the resolvent operator R can be simplified given the restrictions created by the hybridization operator V . For example, the piece $\left[f_1^\dagger t_1 p \right] P$ can only involve states of the form $f^{n+1} p^5 f^n$ since the ground state manifold contains only states of the form $f^n p^6 f^n$. When acting on these states, the resolvent is simplified to an operator that acts only on the states of the rare-earth at site 1

$$R_{f,1} \equiv \sum_{a \in f^{n+1}} \frac{|a\rangle_1 \langle a|_1}{E_{f,a} - E_{f,0} + \Delta_{pf}} \quad (19)$$

where $|a\rangle$ are states of the f^{n+1} configuration and $E_{f,a} - E_{f,0}$ are their energies relative to the f^n ground state, and Δ_{pf} is the atomic potential of the oxygen site. An identical operator $R_{f,2}$ can be defined that acts only on site 2. The innermost resolvent can be simplified in the same way. Here, both rare-earth sites are involved, but the oxygen state is not. It can be replaced by the operator

$$R_{ff}^{(1)} \equiv \sum_{a \in f^{n+1}} \sum_{a' \in f^{n-1}} \frac{|a\rangle_1 \langle a|_1 |a'\rangle_2 \langle a'|_2}{E_{f,a} + E_{f,a'} - 2E_{f,0}}. \quad (20)$$

This allows us to write the process 1 contribution as

$$P \left[p^\dagger t_1^\dagger f_1 \right] R_{f,1} \left[f_2^\dagger t_2 p \right] R_{ff}^{(1)} \left[p^\dagger t_2^\dagger f_2 \right] R_{f,1} \left[f_1^\dagger t_1 p \right] P. \quad (21)$$

Now since the resolvents no longer depend on the oxygen degrees of freedom we can regroup this

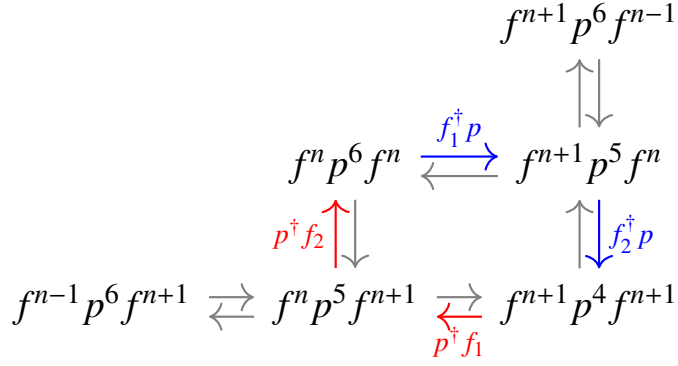


FIG. 2: Process 2 involves intermediate states with two holes on the oxygen site. Scales roughly as $\sim t^4(U_f + \Delta_{pf})^{-2}(2U_f + 2\Delta_{pf} + U_p)^{-1}$

into oxygen and rare-earth parts

$$\sum_{\alpha\beta\mu\nu} \sum_{\alpha'\beta'\mu'\nu'} [P_p P_\alpha^\dagger P_\beta P_\mu^\dagger P_\nu P_p] [P_f f_{1\alpha'} R_{f,1} f_{2\beta'}^\dagger R_{ff}^{(1)} f_{2\mu'} R_{f,1} f_{1\nu'}^\dagger P_f] [t_{1,\alpha\alpha'}^\dagger t_{2,\beta'\beta}^\dagger t_{2,\mu\mu'}^\dagger t_{1,\nu'\nu}], \quad (22)$$

where we have broken up the projector P into rare-earth and oxygen parts as $P \equiv P_p P_f$. The oxygen part is trivial with $P_p P_\alpha^\dagger P_\beta P_\mu^\dagger P_\nu P_p = \delta_{\mu\nu} \delta_{\alpha\beta}$. The final contribution from process 1 is then given by

$$P_f \left(\sum_{\alpha\beta\mu\nu} f_{1\alpha} R_{f,1} f_{2\beta}^\dagger R_{ff}^{(1)} f_{2\mu} R_{f,1} f_{1\nu}^\dagger [t_2 t_1^\dagger]^{\beta\alpha} [t_1 t_2^\dagger]^{\nu\mu} \right) P_f. \quad (23)$$

We carry out the same argument for process 2. Following the arrows in Figure 2 we find the contribution is

$$P [p^\dagger t_2^\dagger f_2] R [p^\dagger t_1^\dagger f_1] R [f_2^\dagger t_2 p] R [f_1^\dagger t_1 p] P. \quad (24)$$

The outermost resolvents can be simplified in the way. The innermost resolvent needs a new definition

$$R_{ff}^{(2)} \equiv \sum_{a \in f^{n+1}} \sum_{a' \in f^{n+1}} \frac{|a\rangle_1 \langle a|_1 |a'\rangle_2 \langle a'|_2}{E_{f,a} + E_{f,a'} - 2E_{f,0} + 2\Delta_{pf} + U_p}, \quad (25)$$

to take into account the additional oxygen holes and Coulomb repulsion in the $f^{n+1} p^4 f^{n+1}$ states, as discussed in the main text. This then gives the operator

$$P [p^\dagger t_2^\dagger f_2] R_{f,2} [p^\dagger t_1^\dagger f_1] R_{ff}^{(2)} [f_2^\dagger t_2 p] R_{f,1} [f_1^\dagger t_1 p] P. \quad (26)$$

Once again we can factor out the oxygen part as

$$\sum_{\alpha\beta\mu\nu} \sum_{\alpha'\beta'\mu'\nu'} [P_p P_\alpha^\dagger P_\beta P_\mu^\dagger P_\nu P_p] [P_f f_{2\alpha'} R_{f,1} f_{1\beta'}^\dagger R_{ff}^{(2)} f_{2\mu'}^\dagger R_{f,1} f_{1\nu'}^\dagger P_f] [t_{2,\alpha\alpha'}^\dagger t_{1,\beta\beta'}^\dagger t_{2,\mu'\mu}^\dagger t_{1,\nu'\nu}]. \quad (27)$$

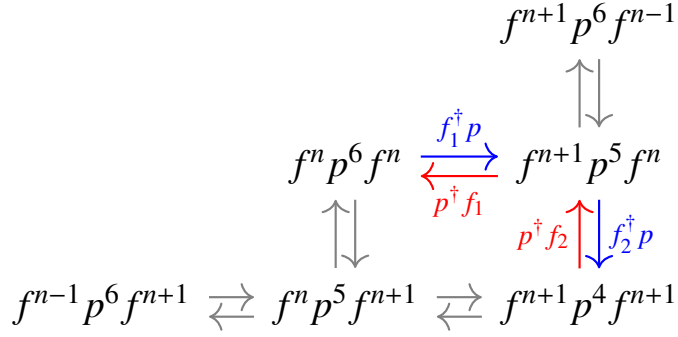


FIG. 3: Process 3 involves intermediate states with only a single hole on the oxygen site. Scales roughly as $\sim t^4(U_f + \Delta_{pf})^{-2}(2U_f + 2\Delta_{pf} + U_p)^{-1}$

The oxygen part is a slightly less trivial this time with $P_p p_\alpha^\dagger p_\beta^\dagger p_\mu p_\nu P_p = \delta_{\beta\mu} \delta_{\alpha\nu} - \delta_{\alpha\mu} \delta_{\beta\nu}$. We thus have

$$P_f \left(\sum_{\alpha\beta\mu\nu} f_{2\alpha} R_{f,2} f_{1\beta} R_{ff}^{(2)} f_{2\mu}^\dagger R_{f,1} f_{1\nu}^\dagger \left([t_2 t_1^\dagger]^{\mu\beta} [t_1 t_2^\dagger]^{\nu\alpha} - [t_2 t_2^\dagger]^{\mu\alpha} [t_1 t_1^\dagger]^{\nu\beta} \right) \right) P_f. \quad (28)$$

Finally, for process 3, we can reuse all of the building blocks that we have put together so far. From Figure 3, we directly write the contribution

$$P \left[p^\dagger t_1^\dagger f_1 \right] R_{f,1} \left[p^\dagger t_2^\dagger f_2 \right] R_{ff}^{(2)} \left[f_2^\dagger t_2 p \right] R_{f,1} \left[f_1^\dagger t_1 p \right] P. \quad (29)$$

Following an identical argument to the previous section we arrive at

$$P_f \left(\sum_{\alpha\beta\mu\nu} f_{1\alpha} R_{f,1} f_{2\beta} R_{ff}^{(2)} f_{2\mu}^\dagger R_{f,1} f_{1\nu}^\dagger \left([t_2 t_2^\dagger]^{\mu\beta} [t_1 t_1^\dagger]^{\nu\alpha} - [t_2 t_1^\dagger]^{\mu\alpha} [t_1 t_2^\dagger]^{\nu\beta} \right) \right) P_f, \quad (30)$$

by simply swapping the site 1 and site 2 labels in part of the exchange path.

MULTIPOLE RANKS AND RESOLVENT OPERATORS

From the expressions above, we see that the interactions between the rare-earth ions can be represented by operators of the form $\sim f_{i,\alpha}^\dagger f_{i,\beta}$ mediated by the oxygens, intermingled with resolvents such as $R_{f,i}$, $R_{ff}^{(1)}$ and $R_{ff}^{(2)}$. As discussed in the main text, we consider the case where the resolvents do not contain the CEF potential and are thus afforded the full spherical symmetry of the free-ion. Because of this symmetry, we can write the resolvents in terms of spherically symmetric projectors into each set of degenerate levels. Expanding out these sums and re-arranging terms, we find that

contributions to each process take the form

$$\sim (f_{1\alpha}^\dagger O_1 f_{1\beta}) (f_{2\mu}^\dagger O_2 f_{2\nu}), \quad (31)$$

where O_1 and O_2 are operators acting on rare-earth sites 1 and 2 built from rank-0 spherically symmetric projectors. The same rank counting outlined in the main text within the charging approximation thus holds true; operators of the form $f_{i,\alpha}^\dagger O_i f_{i,\beta}$ involve multipoles of rank-7 or lower.

CHARGING ENERGY APPROXIMATION

Here we give the details that link the general results to the final expressions for the charging approximation given in the main text. Recall that in this approximation we postulate the energies of the f^n states predominantly depend on the total electron number n . With this approximation we write

$$R_{f,i} \sim \sum_{a \in f^{n+1}} \frac{|a\rangle_i \langle a|_i}{U_f^+ + \Delta_{pf}} \equiv \frac{1 - P_f}{U_f^+ + \Delta_{pf}}, \quad (32)$$

since $E_{f,a} - E_{f,0} \sim U_f^+$ for all states $|a\rangle \in f^{n+1}$. Since the structure of the perturbation forces us to be in the f^{n+1} state, we can extend the sum to all excited states and thus arrive at the projector $1 - P_f$. Applying the same approximation to the innermost resolvents, we find

$$R_{ff}^{(1)} \sim \frac{1 - P_f}{U_f^+ + U_f^-}, \quad R_{ff}^{(2)} \sim \frac{1 - P_f}{2U_f^+ + U_p + 2\Delta_{pf}}, \quad (33)$$

where U_f^- is the energy difference $E_{f,a} - E_{f,0}$ when $|a\rangle$ is a state in the f^{n-1} manifold. We can now use these resolvents to simplify the contributions from the three processes (Figs. 1, 2, and 3) considered earlier, and shown in Eqs. 23, 28, and 30. In each expression the ground state projectors P_f drop out, and we can write the three parts

$$\begin{aligned} 1 : & \frac{1}{(U_f^+ + \Delta_{pf})^2 (U_f^+ + U_f^-)} P_f \left(\sum_{\alpha\beta\mu\nu} f_{1\alpha} f_{2\beta}^\dagger f_{2\mu} f_{1\nu}^\dagger [t_2 t_1^\dagger]^{\beta\alpha} [t_1 t_2^\dagger]^{\nu\mu} \right) P_f, \\ 2 : & \frac{1}{(U_f^+ + \Delta_{pf})^2 (2U_f^+ + U_p + 2\Delta_{pf})} P_f \left(\sum_{\alpha\beta\mu\nu} f_{2\alpha} f_{1\beta} f_{2\mu}^\dagger f_{1\nu}^\dagger \left([t_2 t_1^\dagger]^{\mu\beta} [t_1 t_2^\dagger]^{\nu\alpha} - [t_2 t_2^\dagger]^{\mu\alpha} [t_1 t_1^\dagger]^{\nu\beta} \right) \right) P_f, \\ 3 : & \frac{1}{(U_f^+ + \Delta_{pf})^2 (2U_f^+ + U_p + 2\Delta_{pf})} P_f \left(\sum_{\alpha\beta\mu\nu} f_{1\alpha} f_{2\beta} f_{2\mu}^\dagger f_{1\nu}^\dagger \left([t_2 t_2^\dagger]^{\mu\beta} [t_1 t_1^\dagger]^{\nu\alpha} - [t_2 t_1^\dagger]^{\mu\alpha} [t_1 t_2^\dagger]^{\nu\beta} \right) \right) P_f. \end{aligned}$$

We can further massage the expressions for each process to put the f operators into a standard order. Finally, the swapping of 1 and 2 generates an identical contribution and thus a factor of

two. Collecting the contributions from all three processes and dropping any single-site operators generated by commuting the pieces, we have the final result for H_{eff}

$$H_{\text{eff}} = \sum_{\alpha\beta\mu\nu} (P_{f,1} f_{1\alpha}^\dagger f_{1\beta} P_{f,1}) \mathcal{I}_{12}^{\alpha\beta\mu\nu} (P_{f,2} f_{2\mu}^\dagger f_{2\nu} P_{f,2}), \quad (34)$$

where the interaction matrix is defined as

$$\mathcal{I}_{12}^{\alpha\beta\mu\nu} \equiv \frac{2}{(U_f^+ + \Delta_{pf})^2} \left[\left(\frac{1}{U_f^+ + U_f^-} + \frac{2}{2U_f^+ + U_p + 2\Delta_{pf}} \right) [t_2 t_1^\dagger]^{\mu\beta} [t_1 t_2^\dagger]^{\alpha\nu} - \frac{2 [t_2 t_2^\dagger]^{\mu\nu} [t_1 t_1^\dagger]^{\alpha\beta}}{2U_f^+ + U_p + 2\Delta_{pf}} \right]. \quad (35)$$

as given in the main text. An alternative route to the super-exchange interactions would be to integrate out the oxygen degrees of freedom first. This down-folding gives an effective f - f hopping of order $t_{\text{eff}} \equiv t^2/\Delta_{pf}$. Within the approach discussed here, this corresponds to taking $\Delta_{pf} \gg U_f^\pm$, eliminating all but process 1 at leading order. This then takes the form of a second-order result in the effective hopping t_{eff}

OTHER MICROSCOPIC INTERACTIONS

Here we outline some other possible sources of interactions with the $J = 15/2$ and $J = 8$ manifolds of Dy^{3+} and Ho^{3+} .

Magnetic multipole interactions

Being of magnetostatic origin, the scale of the magnetic multipole interactions (MMI) are simple to address. These are only directly relevant for $\text{Dy}_2\text{Ti}_2\text{O}_7$, as the transverse couplings in non-Kramers doublet relevant for $\text{Ho}_2\text{Ti}_2\text{O}_7$ are time-reversal even. Generally, the scale of the interaction between a rank- K and rank- K' magnetic multipole is approximately given by [13]

$$\mathcal{M}_{KK'} \sim \chi_{K-1} \chi_{K'-1} \langle r^{K-1} \rangle \langle r^{K'-1} \rangle \left(\frac{\mu^{K+K'} \mu_0}{4\pi} \right) \frac{1}{R^{K+K'+1}}, \quad (36)$$

where χ_K is the order K Stevens' parameter [14], $\langle r^K \rangle$ is an atomic radial integral [15], μ is the magnetic moment of the ion and R is the distance between the ions. This expression is somewhat conservative as we have assumed the multipole moments are maximal, including factors of J^K and $J^{K'}$ in $\mu^{K+K'}$ where $J = 15/2$. Projecting into the ground state doublet will quench these moments and further reduce the estimate. This is especially true for $\text{Dy}_2\text{Ti}_2\text{O}_7$ where the ground state

doublet is primarily composed of $|\pm 15/2\rangle$ states and thus has predominantly rank-15 moments that could contribute the transverse couplings. Using $\mu \sim 10 \mu_B$, and we find these MMI are small beyond the dipole-dipole term $\mathcal{M}_{11} \sim 1.4$ K. The more useful number is $D \equiv 4(5\mathcal{M}_{11}/3) \sim 9$ K as discussed in the main text. For dipole-octupole coupling one finds $\mathcal{M}_{13} \sim -16$ mK while for octupole-octupole one finds $\mathcal{M}_{33} \sim 0.17$ mK. Given the factor of $R^{-(K+K'+1)}$, higher-rank interactions are quickly suppressed. The nearest-neighbor dipole-octupole coupling is largest and necessarily projects into exchanges of the form $\sim S_i^z S_j^x + S_i^x S_j^z$. Finally, one must take into account that when the octupole moments are projected into the ground state doublet, their contribution is further reduced. The suppression factors are $\sim \delta/\alpha$, which reduce the dipole-octupole terms by a factor of ~ 0.1 and the octupole-octupole terms by ~ 0.01 . The induced transverse terms after rotation is thus of order $\lesssim 10^{-3}$ mK. The quantum effects are then completely negligible, and thus the MMI can be safely ignored beyond dipole-dipole interactions discussed in the main text.

Electric multipole interactions

Electric multipole interactions (EMI) are only directly relevant for $\text{Ho}_2\text{Ti}_2\text{O}_7$ as the transverse couplings in the Kramers doublet relevant for $\text{Dy}_2\text{Ti}_2\text{O}_7$ are time-reversal odd. Generally, the scale of the EMI between a rank- K and rank- K' electric multipole is approximately given by [16]

$$\mathcal{E}_{KK'} \sim \chi_K \chi_{K'} \langle r^K \rangle \langle r^{K'} \rangle \frac{J^{K+K'}}{R^{K+K'+1}} \left(\frac{e^2}{4\pi\epsilon_0} \right), \quad (37)$$

where e is the elementary charge, ϵ_0 is permittivity of vacuum and the remainder of the notation is the same as in the previous section. We have included factors of J^K and $J^{K'}$ to account for possible matrix element effects as conservatively as possible. The largest of these couplings is the electric quadrupole-quadrupole coupling at order $\mathcal{E}_{22} \sim 63$ mK. Due to the composition of the ground doublet, transverse couplings originating from EMI will carry additional factors of $\sim (\delta/\alpha)^2$, as in the MMI. The scale of these contributions are then $\lesssim 1$ mK. The higher order interactions are even smaller and so the electric multipolar interactions are not a significant source of transverse couplings in $\text{Ho}_2\text{Ti}_2\text{O}_7$.

Lattice mediated interactions

Additional interactions could be mediated through spin-phonon coupling [17]. Due to time-reversal invariance, these can only directly generate interactions between multipoles of even rank.

For $\text{Dy}_2\text{Ti}_2\text{O}_7$ these vanish under projection into the ground state CEF doublet, and thus do not contribute directly to the transverse terms. For $\text{Ho}_2\text{Ti}_2\text{O}_7$, such even-rank interaction can contribute directly to the transverse terms. To evaluate the plausibility of such a scenario, we consider two models of spin-phonon interaction, a site-phonon and bond-phonon model. In the site-phonon model, we consider only the coupling of the on-site multipoles to the local lattice distortion. In the same way as the CEF, when represented as Stevens' operator equivalents, these can only include operators up to rank-6. When the site-phonon is integrated out, these operators are squared so only interactions of rank-12 or less can be generated. In a bond-phonon type model, we imagine the lattice distortion modifying the exchanges already present in the system. Given the argument in the main text, we expect these to be predominantly rank-7 or lower and thus when the phonon is integrated out the induced interactions are rank-14 or smaller. Since these are not the direct rank-16 interactions needed to connect $|\pm 8\rangle$ to $|\mp 8\rangle$, they are suppressed by the sub-leading doublet components by same mechanisms discussed in the main text. Additionally, there will be a further suppression from the energy scale of the phonon that was integrated out. We thus can safely ignore the spin-lattice couplings in our analysis.

Direct exchange

We have accounted for some of the inter-site Coulomb interaction in our treatment of EMI. Other contributions such as direct exchange between the rare-earth ions is likely to be of the same order or smaller given their large separation. Generally, one could write pair-wise direct exchange contributions in the form

$$\sum_{ij} \sum_{\alpha\beta\mu\nu} \mathcal{U}_{ij}^{\alpha\beta\mu\nu} f_{i\alpha}^\dagger f_{i\beta} f_{j\mu}^\dagger f_{j\nu} \quad (38)$$

As we have seen, the one-electron form of the operators at each site restrict this to generate multipolar interactions of rank-7 or less. Thus we have the same suppression factor $(\delta/\alpha)^2$ as discussed in the main text. Given the scale of the EMI, we then expect these terms to be negligible. We note that direct exchange interactions between the rare-earth and oxygen sites could be present. However, due to the need to include additional electron transfers to generate interactions and the filled shell of the oxygen site, we would not expect these terms to be important.

-
- [1] M. J. Harris, S. T. Bramwell, D. F. McMorrow, T. Zeiske, and K. W. Godfrey, “Geometrical frustration in the ferromagnetic pyrochlore $\text{Ho}_2\text{Ti}_2\text{O}_7$,” *Phys. Rev. Lett.* **79**, 2554 (1997).
- [2] S. Rosenkranz, A. P. Ramirez, A. Hayashi, R. J. Cava, R. Siddharthan, and B. S. Shastry, “Crystal-field interaction in the pyrochlore magnet $\text{Ho}_2\text{Ti}_2\text{O}_7$,” *J. Appl. Phys.* **87**, 5914 (2000).
- [3] O. A. Petrenko, M. R. Lees, and G. Balakrishnan, “Magnetization process in the spin-ice compound $\text{Ho}_2\text{Ti}_2\text{O}_7$,” *Phys. Rev. B* **68**, 012406 (2003).
- [4] DP Leusink, F Coneri, M Hoek, S Turner, H Idrissi, G Van Tendeloo, and H Hilgenkamp, “Thin films of the spin ice compound $\text{Ho}_2\text{Ti}_2\text{O}_7$,” *APL Materials* **2**, 032101 (2014).
- [5] A. Bertin, Y. Chapuis, P. Dalmas de Réotier, and A. Yaouanc, “Crystal electric field in the $\text{R}_2\text{Ti}_2\text{O}_7$ pyrochlore compounds,” *J. Phys. Condens. Matter* **24**, 256003 (2012).
- [6] H. Fukazawa, R. G. Melko, R. Higashinaka, Y. Maeno, and M. J. P. Gingras, “Magnetic anisotropy of the spin-ice compound $\text{Dy}_2\text{Ti}_2\text{O}_7$,” *Phys. Rev. B* **65**, 054410 (2002).
- [7] S. Onoda and Y. Tanaka, “Quantum fluctuations in the effective pseudospin- $\frac{1}{2}$ model for magnetic pyrochlore oxides,” *Phys. Rev. B* **83**, 094411 (2011).
- [8] K. A. Ross, L. Savary, B. D. Gaulin, and L. Balents, “Quantum excitations in quantum spin ice,” *Phys. Rev. X* **1**, 021002 (2011).
- [9] S. Lee, S. Onoda, and L. Balents, “Generic quantum spin ice,” *Phys. Rev. B* **86**, 104412 (2012).
- [10] S. T. Bramwell, M. J. Harris, B. C. den Hertog, M. J. P. Gingras, J. S. Gardner, D. F. McMorrow, A. R. Wildes, A. L. Cornelius, J. D. M. Champion, R. G. Melko, *et al.*, “Spin correlations in $\text{Ho}_2\text{Ti}_2\text{O}_7$: a dipolar spin ice system,” *Phys. Rev. Lett.* **87**, 047205 (2001).
- [11] R. G. Melko, B. C. den Hertog, and M. J. P. Gingras, “Long-range order at low temperatures in dipolar spin ice,” *Phys. Rev. Lett.* **87**, 067203 (2001).
- [12] I. Lindgren, “The Rayleigh-Schrodinger perturbation and the linked-diagram theorem for a multi-configurational model space,” *J. Phys. B: At. Mol.* **7**, 2441 (1974).
- [13] J. M. Baker, “Interactions between ions with orbital angular momentum in insulators,” *Rep. Prog. Phys.* **34**, 109 (1971).
- [14] K. W. H. Stevens, “Matrix elements and operator equivalents connected with the magnetic properties of rare earth ions,” *Proc. Phys. Soc. A* **65**, 209 (1952).

- [15] A. J. Freeman and J. P. Desclaux, “Dirac-Fock studies of some electronic properties of rare-earth ions,” *J. Magn. Magn. Mater.* **12**, 11 (1979).
- [16] W. P. Wolf and R. J. Birgeneau, “Electric multipole interactions between rare-earth ions,” *Phys. Rev.* **166**, 376 (1968).
- [17] O. Tchernyshyov and G. Chern, “Spin-lattice coupling in frustrated antiferromagnets,” in *Introduction to Frustrated Magnetism* (Springer, 2011) pp. 269–291.